

Global Optimization on Graph-Structured Data via Gaussian Processes with Spectral Representations

Shu Hong* Yongsheng Mei* Mahdi Imani† Tian Lan*

Abstract

Bayesian optimization (BO) is a powerful framework for optimizing expensive black-box objectives, yet extending it to graph-structured domains remains challenging due to the discrete and combinatorial nature of graphs. Existing approaches often rely on either full graph topology—impractical for large or partially observed graphs—or incremental exploration, which can lead to slow convergence. We introduce a scalable framework for global optimization over graphs that employs low-rank spectral representations to build Gaussian process (GP) surrogates from sparse structural observations. The method jointly infers graph structure and node representations through learnable embeddings, enabling efficient global search and principled uncertainty estimation even with limited data. We also provide theoretical analysis establishing conditions for accurate recovery of underlying graph structure under different sampling regimes. Experiments on synthetic and real-world datasets demonstrate that our approach achieves faster convergence and improved optimization performance compared to prior methods.

1 Introduction

Many real-world decision-making tasks involve optimizing an unknown function defined over the node set of a graph [1]. In these settings, each node corresponds to a potential action or configuration, and the goal is to identify the node (or set of nodes) that optimizes a costly-to-evaluate objective. Such problems arise across diverse domains: selecting influential users in social networks for information diffusion, identifying promising molecules in chemical graphs for drug discovery, detecting vulnerable components in power grids, or choosing effective interventions in neural connectivity graphs. A key challenge across these graph-based optimization is that evaluating the unknown function at each node – via sampling, simulation, or physical experimentation – is often expensive. Therefore, it is essential to leverage structural correlations and latent biases encoded in the underlying graph topology to facilitate efficient search and optimization, using limited observations.

Bayesian optimization (BO) [2, 3, 4, 5] is a sequential optimization technique tailored for optimizing expensive-to-evaluate black-box functions. It typically employs Gaussian Processes (GPs) as probabilistic surrogate models, providing uncertainty-aware predictions at unobserved points to guide evaluations toward regions of promising or uncertain outcomes. However, conventional GP models and kernels assume continuous Euclidean input spaces, complicating their adaptation to discrete, graph-structured data. Existing GP-based approaches to graph optimization can be grouped into three categories, kernel-based BO [6, 7, 1], embedding-driven BO [6], and combinatorial BO [8, 9]. They typically require complete graph observability – a requirement rarely satisfied in practical, partially observed scenarios. Recent graph-specific BO methods [1] partially address this by incrementally modeling and exploring local graph neighborhoods. Such method is limited to making only local improvements in the optimization process by incrementally discovering and modeling new neighboring subgraphs. They fail to leverage global structural features and result in extensive local evaluations and slow convergence. To the best of our knowledge, no existing BO framework addresses the challenge of scalable global optimization of unknown functions on large, partially observed graphs.

*Shu Hong and Tian Lan are with George Washington University, United States (e-mail: shu.hong@gwu.edu, tlan@gwu.edu). Yongsheng Mei is with Amazon (e-mail: ysmei97@gmail.com). Mahdi Imani is with Northeastern University, United States (e-mail: m.imani@northeastern.edu).

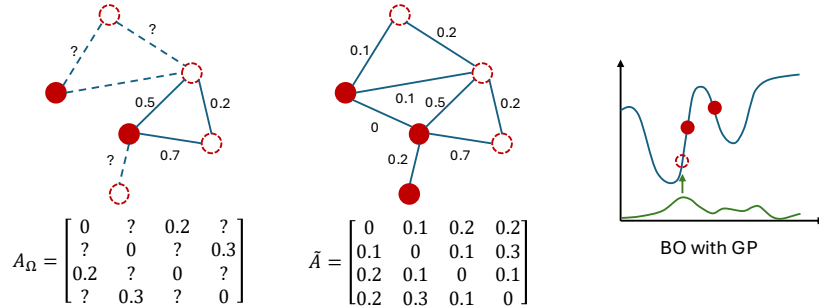


Figure 1: Illustration of the proposed global Bayesian optimization (BO) framework on graphs.

We propose a novel global BO framework on graph data using GP models enabled by low-rank approximations and graph spectral drawing, as illustrated in Fig. 1. Our key insight is that real-world graphs often exhibit structured connectivity patterns — driven by latent factors such as community affiliation in social networks, node dependence in transportation networks, or functional properties in molecular graphs. These induce low-rank properties in the underlying graphs' adjacency matrices [10, 11] and can be leveraged for develop a global surrogate model of the unknown function on graph, from limited edge samples [12, 13]. More precisely, our approach first employs a neural matrix completion model to infer a global surrogate of the adjacency matrix from sparse edge observations. From this surrogate, we compute spectral embeddings that represent graph nodes in a low-dimensional Euclidean space, preserving global topology. Finally, we perform Gaussian Process-based Bayesian optimization in this embedding space to guide sample-efficient global search. We support our method with rigorous theoretical guarantees for accurate graph reconstruction, ensuring robustness under both random and deterministic edge sampling strategies. We prove that, under standard incoherence assumptions, the true graph adjacency matrix can be recovered exactly from a near-optimal number of randomly sampled edges. We establish analogous guarantees for deterministic sampling patterns based on the spectral properties of the observation pattern. We also demonstrate strong empirical performance across diverse graph benchmarks.

Our main contributions are summarized as follows:

- **BO for Graph Data:** We introduce a principled methodological framework that integrates low-rank matrix completion, spectral graph embedding, and global Bayesian optimization, enabling efficient optimization on large, partially observed graphs.
- **Theoretical Guarantees:** We provide non-asymptotic sample complexity bounds for accurate graph structure recovery under both random and deterministic sampling strategies, establishing conditions under which our method is provably effective.
- **Scalable Algorithms:** We develop neural network-based parameterizations to efficiently compute the surrogate graph and its spectral embeddings from partial observations and samples. This online spectral computation enables scalable global exploration and optimization on large graphs while preserving key structural properties.
- **Empirical Evaluation:** We validate our method on diverse synthetic and real-world graph datasets, demonstrating consistent improvements in sample efficiency and optimization performance over existing graph BO and search baselines.

2 Related Work

Bayesian Optimization on Graphs BO is a sample-efficient strategy for optimizing expensive-to-evaluate unknown functions. While traditionally applied to continuous Euclidean domains, recent work on graph-based BO include kernel-

based methods using structural priors [1, 14], deep learning-based graph embeddings for node-level optimization [6], and combinatorial methods using graph Cartesian products [8]. Approaches specifically designed for Neural Architecture Search (NAS) encode architectures as fully observable graph structures [15, 16, 7, 9], while others focus on optimizing functions over subsets of nodes or employing shortest-path encodings [17, 18, 19]. However, these existing methods either assume full graph observability or explicitly defined combinatorial structures or rely on incremental local exploration. In contrast, we consider construct global surrogate models from partial observations to enable global BO on graph data.

Matrix Completion for Graph Structure Recovery Matrix completion reconstructs low-rank matrices from partial observations under assumptions such as incoherence and sufficient sampling [12, 20]. In graph analytics, it provides a principled method to infer missing edges and approximate true graph structures from partially observed adjacency matrices. Recent advances provide robust deterministic guarantees under general conditions, reinforcing its practical utility [21]. In our work, low-rank matrix completion is leveraged to recover incomplete graph topologies, forming the surrogate structures essential for subsequent spectral embedding and GP modeling in large-scale optimization scenarios.

Spectral Embedding for Graph-based Learning Spectral embedding techniques, such as Laplacian Eigenmaps [22], spectral clustering [23], and diffusion maps [24], provide low-dimensional node representations that preserve local and global graph structure. Building on these foundations, the graph-kernel literature introduced diffusion kernels on graphs [25, 26], enabling GP to model functions over nodes with principled uncertainty estimates. More recent works have incorporated spectral priors into deep reinforcement learning and structured bandits [27, 28], but few have directly constructed GP surrogates from learned embeddings. Our approach closes this gap by using neural low-rank and spectral embeddings to define a graph-informed GP kernel, yielding both scalable inference and reliable uncertainty quantification.

3 Problem Statement

We consider optimizing an expensive-to-evaluate black-box function defined over nodes of a large, partially observed graph whose full structure is initially unknown. Formally, let $G = (\mathcal{V}, \mathcal{E})$ denote an undirected weighted graph, where $\mathcal{V} = \{1, \dots, n\}$ is the set of nodes, and edges $\mathcal{E} = \{(i, j) \in \mathcal{V} \times \mathcal{V} \mid A_{ij} > 0\}$ are determined by an unknown symmetric adjacency matrix $A \in [0, 1]^{n \times n}$. The entries $A_{ij} > 0$ indicate connected nodes, whereas $A_{ij} = 0$ means nodes i and j are disconnected.

Evaluating the black-box function $y : \mathcal{V} \rightarrow \mathbb{R}$ at each node is costly, typically due to computationally intensive simulations or laboratory experiments—for instance, molecular property prediction in drug discovery or evaluating influence spread in social networks. Our goal is to identify the globally optimal node:

$$v^* = \arg \max_{v \in \mathcal{V}} y(v).$$

In practice, we can query $y(v)$ only at only a small subset of nodes, introducing two intertwined challenges. First, partial observability of the graph hinders navigation of the large, discrete node space, since most optimizers assume full topology. Second, each node evaluation is expensive, severely constraining the query budget and necessitating optimization strategies capable of efficiently utilizing sparse structural cues to quickly identify promising nodes.

4 Methodology

Our method addresses the challenges outlined in the previous section through a principled iterative optimization framework tailored specifically for partially observed graphs. At each iteration, our approach simultaneously samples informative edges and selectively queries node functions. Our framework integrates two key modeling components: (i) *low-rank matrix completion*, which reconstructs a global surrogate adjacency matrix from partial edge observations,

and (ii) *spectral graph embeddings*, which facilitate Gaussian Process-based Bayesian optimization in a continuous embedding space.

Formally, at each iteration t , we maintain two sets of partial observations: $\Omega^{(t)} \subseteq \mathcal{V} \times \mathcal{V}$ and $\mathcal{V}^{(t)} \subseteq \mathcal{V}$, where $\Omega^{(t)}$ comprises pairs of nodes whose edge connectivity status is known, and $\mathcal{V}^{(t)}$ contains nodes whose function values have been queried so far. The corresponding partially observed adjacency matrix $A_{\Omega}^{(t)}$ is defined by the projection operator $\mathcal{P}_{\Omega}^{(t)} : \mathbb{R}^{n \times n} \rightarrow \mathbb{R}^{n \times n}$, given by:

$$[\mathcal{P}_{\Omega}^{(t)}(A)]_{ij} = \begin{cases} A_{ij}, & (i, j) \in \Omega^{(t)}, \\ 0, & \text{otherwise.} \end{cases}$$

We initially focus on a noise-free setting, meaning the observed entries in $A_{\Omega}^{(t)}$ accurately reflect the true underlying graph structure; however, our methodology can be readily generalized to noisy scenarios. In parallel, at each iteration t , we query the function value at one selected node $v \in \mathcal{V}$; this procedure naturally generalizes to querying multiple nodes simultaneously (batch queries).

Our iterative optimization targets two complementary objectives at each iteration:

1. **Graph Reconstruction:** Leveraging the currently observed edges $\Omega^{(t)}$, we efficiently reconstruct a low-rank approximation $\tilde{A}^{(t)}$ of the unknown adjacency matrix A . This surrogate adjacency matrix globally captures structural patterns critical for accurate graph modeling.
2. **Bayesian Optimization via Spectral Embedding:** Utilizing the reconstructed surrogate graph $\tilde{A}^{(t)}$, we compute spectral node embeddings to derive a continuous representation of nodes. We then fit a GP surrogate model in this embedding space and strategically select the next node for evaluation via principled BO acquisition strategies, thereby guiding our search toward the globally optimal node.

By iteratively refining both the surrogate graph structure and node embeddings based on cumulative partial observations, our method effectively navigates the exploration-exploitation trade-off inherent in BO. It enables efficient global optimization despite the initial uncertainty and limited query budget. The complete iterative procedure of our method is summarized in Algorithm 1, while our balanced edge-sampling strategy is detailed separately in Algorithm 2. We now provide a detailed elaboration on each of these methodological components.

4.1 Matrix Completion and Spectral Embedding

To address the challenge of partial graph observability, we first reconstruct the unknown adjacency matrix through a low-rank matrix completion formulation. Subsequently, we derive spectral embeddings from this reconstructed graph to accurately capture the global graph geometry. These embeddings enable the smooth modeling of function values, essential for guiding efficient BO. The reconstruction and embedding steps are jointly optimized via stochastic gradient descent (SGD), ensuring that the gradually revealed graph structure directly informs our embedding representations.

4.1.1 Rank-constrained Matrix Completion.

At any iteration, given a partially observed adjacency matrix A_{Ω} , we aim to reconstruct the full adjacency matrix A . To achieve this, we seek a low-rank surrogate \tilde{A} that accurately approximates the true adjacency structure on observed edges. Directly imposing a low-rank constraint (e.g., $\text{rank}(\tilde{A}) \leq d$) leads to a computationally intractable, non-convex optimization problem. Therefore, we adopt the convex relaxation via nuclear-norm regularization [12, 20], formulating the optimization problem as:

$$\min_{\tilde{A} \in \mathbb{R}^{n \times n}, \tilde{A} = \tilde{A}^{\top}} L_1 = \frac{1}{|\Omega|} \|P_{\Omega}(\tilde{A} - A_{\Omega})\|_F^2 + \tau \|\tilde{A}\|_*, \quad (1)$$

where τ is a regularization parameter. The nuclear norm $\|\tilde{A}\|_* = \sum_{i=1}^n \kappa_i(\tilde{A}) = \sum_{i=1}^n |\gamma_i(\tilde{A})|$, summing singular values κ_i . Since \tilde{A} is symmetric, its singular values equals the absolute values of its eigenvalues γ_i , thus the nuclear norm implicitly induces low-rank solutions. Without the nuclear-norm term, the recovery will be underdetermined, as infinitely many completions match the observed entries.

Algorithm 1 Global Graph BO via Low-Rank Completion and Spectral Embedding

Input: Graph $G = (\mathcal{V}, \mathcal{E})$ with adjacency matrix A , total iterations T , initial sample size N_0

Parameter: Rank budget d_1 , embedding dimension d_2 , acquisition function $\mathcal{A}(\cdot)$, neural networks Q_θ and F_θ , regularization weights $(\tau, \mu_2, \mu_Q, \mu_F)$, batch sizes (B_1, B_2, B_3) , learning rates $(\eta_Q, \eta_\Gamma, \eta_F)$

Output: Estimated optimizer v^*

```

1: Randomly sample initial nodes  $\mathcal{V}^{(0)} \subset \mathcal{V}$ ,  $|\mathcal{V}^{(0)}| = N_0$ 
2: Query  $y(v)$  for all  $v \in \mathcal{V}^{(0)}$ 
3: Initialize observed edge set  $\Omega^{(0)}$ , neural parameters  $(\theta_Q, \theta_F)$ , eigenvalues  $\Gamma$ 
4: for  $t = 1$  to  $T$  do
5:   (A) Update Surrogate Graph and Embedding:
6:   for each SGD epoch do
7:     Sample (observed) edges  $\mathcal{B}_1 \sim \text{Unif}(\Omega^{(t)}, B_1)$ 
8:     Sample node pairs  $\mathcal{B}_2 \sim p_{\tilde{A}}$  of size  $B_2$ 
9:     Sample nodes  $\mathcal{B}_3 \sim \text{Unif}(\mathcal{V}, B_3)$ 
10:    Compute batch losses  $\hat{L}_1, \hat{L}_2, \hat{L}_{\text{ortho1}}, \hat{L}_{\text{ortho2}}$ 
11:    Update  $(\theta_Q, \theta_F, \Gamma)$  via gradient descent on total loss  $\hat{\mathcal{L}} = \hat{L}_1 + \mu_2 \hat{L}_2 + \mu_Q \hat{L}_{\text{ortho1}} + \mu_F \hat{L}_{\text{ortho2}}$ 
12:   end for
13:   (B) GP and Acquisition:
14:   Extract embeddings  $F_\theta$ 
15:   Construct kernel  $k(u, v)$  via eigenpairs of  $\tilde{L}$ 
16:   Fit GP on  $\{(v, y(v)) : v \in \mathcal{V}^{(t)}\}$ 
17:   Select  $v^{(t+1)} = \arg \max_{v \in \mathcal{V}} \mathcal{A}(v)$ 
18:   Query  $y(v^{(t+1)})$ ; update  $\mathcal{V}^{(t+1)} \leftarrow \mathcal{V}^{(t)} \cup \{v^{(t+1)}\}$ 
19:   (C) Edge Sampling:
20:   Update  $\Omega^{(t+1)}$  via Algorithm 2
21: end for
22: return  $v^* = \arg \max_{v \in \mathcal{V}^{(T)}} y(v)$ 

```

4.1.2 Theoretical Guarantees and Sampling Complexity.

We summarize theoretical guarantees for exact recovery under both random and deterministic sampling conditions as follows.

Theorem 1 (Random Sampling). *Let $A \in \mathbb{R}^{n \times n}$ be symmetric, $\text{rank}(A) = r$, and μ -incoherent: $\max_i \|Q_{i,:}\|_2^2 \leq \mu r/n$ for the eigen-basis $A = Q\Gamma Q^\top$. Sample each entry independently with probability $p = |\Omega|/n^2$. There exist constants $C, c, c' > 0$ such that if $|\Omega| \geq C\mu r n \log^2 n$, the solution of Problem (1) with $0 < \tau \leq \min(c\frac{p}{\sqrt{r}}, c'\frac{1}{n})$ is unique and exactly recovers $\tilde{A}^* = A$ with high probability.*

Theorem 2 (Deterministic Sampling). *Let A satisfy the same conditions as in Theorem 1 and let Ω be an arbitrary index set. Form the observation graph $\tilde{G} = (\mathcal{V}, \Omega)$ and let average degree $\bar{d} = \frac{2|\Omega|}{n}$, $\xi_{\tilde{G}} = \bar{d} - \lambda_2(A_\Omega)$, $\varphi_{\tilde{G}} = \max_{u \in \mathcal{V}} |\deg(u) - \bar{d}|$. There exist constants $C, c > 0$ such that if $\alpha = \frac{\mu r n}{|\Omega|}(\xi_{\tilde{G}} + \varphi_{\tilde{G}}) < \frac{1}{3}$ and $|\Omega| \geq C\mu r n(2\xi_{\tilde{G}} + \varphi_{\tilde{G}})$, the solution of Problem (1) with $0 < \tau \leq \frac{c|\Omega|}{n^2\sqrt{r}}$ is unique and exactly recovers the $\tilde{A}^* = A$ with high probability.*

Remark 1 (Link to Algorithm 2). *Theorems 1 and 2 hinge on controlling the two graph-statistics $\varphi_{\tilde{G}}$ and $\xi_{\tilde{G}}$ so that for sampling efficiency. Algorithm 2 realises this in two complementary phases: (A) **Seed expansion**: Repeatedly attaches the current seed node (either $v^{(t+1)}$ or $v^{(t+1)*}$) to the under-sampled neighbor u^* with largest degree deficit $\bar{d} - d(u)$, directly shrinking the degree-imbalance $\varphi_{\tilde{G}}$. (B) **Uniform re-balancing**: Sprinkles the remaining budget uniformly at random over all unobserved edges, which with high probability restores the spectral gap to $\xi_{\tilde{G}} = \Theta(pn)$. Together with the reduced $\varphi_{\tilde{G}}$, this guarantees $|\Omega| \gtrsim \mu r n \log^2 n$.*

Algorithm 2 Balanced Edge Sampling

Inputs: Current observation set Ω , newly queried node $v^{(t+1)}$, current best node $v^{(t+1)*}$, edge sample budget Q , balance fraction $0 < \beta < 1$, exploration probability $0 < \varepsilon < 1$

Output: Updated observation set $\Omega^{(t+1)}$

- 1: Compute current degrees $d(u) = |\{v : (u, v) \in \Omega\}|$ and average $\bar{d} = \frac{1}{n} \sum_u d(u)$.
- 2: **(A) Seed expansion:**
- 3: $Q_1 \leftarrow \lceil \beta Q \rceil$, $\Omega_A \leftarrow \emptyset$
- 4: **for** $k = 1$ to Q_1 **do**
- 5: Set $v_{\text{seed}} \leftarrow v^{(t+1)}$ with probability ε and $v_{\text{seed}} \leftarrow v^{(t+1)*}$ otherwise
- 6: Candidate set $\mathcal{U} = \{u \neq v_{\text{seed}} \mid (u_{\text{seed}}, v) \notin \Omega \cup \Omega_A\}$
- 7: For every $u \in \mathcal{U}$ compute degree deficit $\Delta(u) = |\bar{d} - d(u)|$
- 8: Select $u^* = \arg \max_{u \in \mathcal{U}} \Delta(u)$
- 9: $\Omega_A \leftarrow \Omega_A \cup \{(v_{\text{seed}}, u^*)\}$
- 10: $d(v_{\text{seed}}) \leftarrow d(v_{\text{seed}}) + 1$, $d(u^*) \leftarrow d(u^*) + 1$
- 11: **end for**
- 12: **(B) Re-balancing**
- 13: $Q_2 \leftarrow Q - Q_1$, $\Omega_B \leftarrow \emptyset$
- 14: $R \leftarrow \{(u, v) \notin \Omega \cup \Omega_A, u < v\}$
- 15: Sample Q_2 edges uniformly without replacement from R into Ω_B
- 16: $\Omega^{(t+1)} \leftarrow \Omega \cup \Omega_A \cup \Omega_B$
- 17: **return** $\Omega^{(t+1)}$

Thus Algorithm 2 is a practical instantiation of the deterministic-sampling conditions in Theorem 2, achieving the same minimax sample-complexity $O(\mu r n \log^2 n)$ as the random sampling while biasing early queries toward nodes of interest.

The nuclear-norm problem (1) can in theory be solved using Singular Value Thresholding (SVT), yet with complexity $\mathcal{O}(n^3)$ at each iteration. Instead, we leverage a truncated eigendecomposition of rank $d_1 \ll n$ to replace each SVT step. By Eckart–Young–Mirsky theorem [29], this yields the best rank- d_1 approximation in Frobenius norm and costs $\mathcal{O}(d_1 n^2)$.

4.1.3 Spectral parameterization.

To enforce low-rank structure while retaining scalability, we parameterize the surrogate adjacency \tilde{A} via a truncated spectral decomposition. We choose the budget rank $d_1 \ll n$, either based on the known ground-truth rank r (if available), or set according to computational and memory budgets. Formally, we approximate \tilde{A} through its top d_1 eigenpairs:

$$\tilde{A} = \sum_{i=1}^{d_1} \gamma_i q_i q_i^\top = Q \Gamma Q^\top, \quad (2)$$

where $Q = [q_1, \dots, q_{d_1}] \in \mathbb{R}^{n \times d_1}$ contains orthonormal eigenvectors $\{q_i\}_{i=1}^{d_1}$ satisfying $Q^\top Q = I_{d_1}$. $\Gamma = \text{diag}(\gamma_1, \dots, \gamma_{d_1})$ holds the corresponding eigenvalues. By construction, \tilde{A} is explicitly symmetric with $\text{rank}(\tilde{A}) \leq d_1$, and we only store $\mathcal{O}(nd_1)$ entries rather than $\mathcal{O}(n^2)$ for a full eigen-decomposition.

Due to the nuclear-norm regularization in Problem (1), the solution naturally encourages a low-rank structure. Consequently, the truncated spectral representation (2) not only enforces symmetry and $\text{rank}(\tilde{A}) \leq d_1$ but typically yields an effective rank well below the budgeted rank d_1 .

Substituting $\tilde{A} = Q\Gamma Q^\top$ into (1) gives the spectral loss $L_1(\Gamma, Q)$ as:

$$L_1 = \frac{\sum_{(u,v) \sim \Omega} \left(\sum_{i=1}^{d_1} \gamma_i q_i(u) q_i(v) - A_{uv} \right)^2}{|\Omega|} + \tau \sum_{i=1}^{d_1} |\gamma_i|, \quad (3)$$

subject to $Q^\top Q = I_{d_1}$. Here, the summation runs over all observed edges $(u, v) \in \Omega$, and A_{uv} denotes the observed adjacency values. Although (3) is non-convex (in Q) and non-smooth (in Γ), it can be solved efficiently in practice using proximal soft-thresholding gradient descent on Γ and soft orthonormality constraints on Q .

4.1.4 Spectral Graph Drawing for Downstream GP Modeling.

To effectively apply GP-based BO on graphs, we must define a graph-aware kernel (covariance function) that accurately captures relationships among nodes. Specifically, we leverage spectral embeddings derived from the surrogate adjacency matrix \tilde{A} and embed nodes into a low-dimensional Euclidean space. Intuitively, stronger connectivity in \tilde{A} should pull node embeddings closer, yielding a smooth function modeling for the GP.

Let $\tilde{d}(u) = \sum_{v \in \mathcal{V}} \tilde{A}(u, v)$ be the degree of vertex u in the current surrogate graph and $D = \text{diag}(\tilde{d}(1), \dots, \tilde{d}(n))$. Define $\tilde{L} = I - D^{-1/2} \tilde{A} D^{-1/2}$ as the normalized Laplacian. We choose an embedding dimension d_2 (typically $d_2 \leq d_1 \ll n$) and let $F = \{f_1, \dots, f_{d_2}\} \in \mathbb{R}^{n \times d_2}$ be the matrix of the d_2 eigenvectors of \tilde{L} corresponding to the smallest non-zero eigenvalues. Enforcing $F^\top F = I_{d_2}$ ensures an orthonormal embedding basis in \mathbb{R}^{d_2} .

Equivalently, we can view these eigenvectors as the solution to the spectral smoothness problem:

$$\begin{aligned} L_2(F, \tilde{A}) &= \text{tr}(F^\top \tilde{L} F) \\ &= \frac{1}{2} \sum_{(u,v) \in \mathcal{V} \times \mathcal{V}} \tilde{A}(u, v) \|D(u)^{-\frac{1}{2}} f(u) - D(v)^{-\frac{1}{2}} f(v)\|_2^2 \\ &= \frac{1}{2} \sum_{(u,v) \in \mathcal{V} \times \mathcal{V}} \tilde{A}(u, v) \sum_{i=1}^{d_2} \left(D(u)^{-\frac{1}{2}} f_i(u) - D(v)^{-\frac{1}{2}} f_i(v) \right)^2, \end{aligned} \quad (4)$$

subject to $F^\top F = I_{d_2}$. Notice that L_2 is summed over all node pairs as spectral smoothness should cover the whole surrogate graph \tilde{A} . Minimizing $\text{tr}(F^\top \tilde{L} F)$ forces F onto the span of the d_2 lowest non-zero eigenvectors of \tilde{L} . The following lemma clarifies the optimality property.

Lemma 1. *The minimum of the loss L_2 is achieved when the solved eigenvectors $\{f_i\}_{i=1}^{d_2}$ correspond to the d_2 smallest non-zero eigenvalues of the surrogate Laplacian \tilde{L} .*

Remark 2 (Different choices of d_1 and d_2). *Rank budget d_1 in (2) controls the maximum rank of the surrogate adjacency \tilde{A} and thus the degrees of freedom for reconstructing missing edges. Its effective value is driven by the observed pattern Ω . d_2 is the embedding dimension for the downstream GP model: larger d_2 can capture finer graph geometry at the cost of higher GP complexity $\mathcal{O}(nd_2^2)$.*

4.1.5 Joint Optimization via Neural Network Representations.

In this section, we describe a scalable framework to jointly optimize the objectives of graph reconstruction, spectral embedding smoothness, and eigenvector orthonormality constraints via neural network parameterizations and stochastic gradient methods. Such joint optimization efficiently approximates the eigenbasis of the surrogate graph Laplacian, providing stable and computationally feasible embeddings for large-scale graphs observed incrementally.

Formally, our combined optimization objective integrates matrix completion loss $L_1(\Gamma, Q)$, spectral smoothness loss $L_2(F, \tilde{A})$, and soft orthonormality constraints:

$$\min_{\Gamma, Q, F} L_1(\Gamma, Q) + \mu_2 L_2(F, \tilde{A}) + \mu_Q L_{\text{ortho1}}(Q) + \mu_F L_{\text{ortho2}}(F), \quad (5)$$

where L_1 and L_2 are defined in equations (3) and (4), respectively. The soft orthonormality constraints $L_{\text{ortho1}}(Q) = \|Q^\top Q - I_{d_1}\|_F^2$ and $L_{\text{ortho2}}(F) = \|F^\top F - I_{d_2}\|_F^2$ encourage approximate orthonormality of the eigenvectors.

Neural network parameterizations. Directly computing eigenvectors for large-scale graphs is computationally prohibitive. Thus, we parameterize eigenvectors Q and F as outputs of neural networks with parameters θ , denoted as Q_θ and F_θ . We employ SGD using carefully designed mini-batch sampling schemes for scalability. For L_1 , we sample a mini-batch of edges $\mathcal{B}_1 = \{(u_k, v_k, A_{u_k v_k})\}_{k=1}^{B_1}$ from the observed set Ω at each training epoch. For L_2 , directly sampling edges (u, v) from the full $n \times n$ adjacency matrix \tilde{A} is of complexity $\mathcal{O}(n^2)$, which is computationally expensive for large graphs. Instead, we let $p_{\tilde{A}} = \frac{\tilde{A}(u, v)}{\sum_{(x, y) \in \mathcal{V} \times \mathcal{V}} \tilde{A}(x, y)}(u, v) \propto \tilde{A}(u, v)$ as a mixture of d_1 rank-one components and rewrite

$$L_2 = \mathbb{E}_{(u, v) \in p_{\tilde{A}}} \sum_{i=1}^{d_2} \left(D(u)^{-\frac{1}{2}} f_i(u) - D(v)^{-\frac{1}{2}} f_i(v) \right)^2.$$

Each SGD draw is then: (1) Sample $i \in \{1, \dots, d_1\}$ with probability $w_i = \frac{\sum_{u, v} \gamma_i q_i(u) q_i(v)}{\sum_{j, u, v} \gamma_j q_j(u) q_j(v)} = \frac{|\gamma_i|}{\sum_j |\gamma_j|}$. (2) Independently sample $u \sim \frac{|q_i(u)|}{\sum_x |q_i(x)|}$, $v \sim \frac{|q_i(v)|}{\sum_x |q_i(x)|}$. By simple algebra, we can show such sampling reproduces the joint mass $p_{\tilde{A}}$ exactly, at a sampling cost of $\mathcal{O}(d_1)$. This makes SGD on L_2 scalable to large-scale graphs.

Empirical mini-batch loss functions. The complete optimization objective over the eigen-decomposition $\{q_i, \gamma_i\}_{i=1}^{d_1}$ and $\{f_i\}_{i=1}^{d_2}$ becomes:

$$\min_{\theta, \{\gamma_i\}_{i=1}^{d_1}} \hat{L}_1 + \mu_2 \hat{L}_2 + \mu_Q \hat{L}_{\text{ortho1}} + \mu_F \hat{L}_{\text{ortho2}}, \quad (6)$$

with the following unbiased batch-wise losses: $\hat{L}_1 = \frac{1}{B_1} \sum_{(u, v) \in \mathcal{B}_1} \left(\sum_{i=1}^{d_1} \gamma_i q_i(u) q_i(v) - A_{uv} \right)^2 + \tau \sum_{i=1}^{d_1} |\gamma_i|$, $\hat{L}_2 = \frac{\sum_{(i, j) \in \mathcal{V} \times \mathcal{V}} \tilde{A}_{ij}}{2B_2} \sum_{(u, v) \in \mathcal{B}_2} \|D(u)^{-\frac{1}{2}} F_\theta(u) - D(v)^{-\frac{1}{2}} F_\theta(v)\|_2^2$, $\hat{L}_{\text{ortho1}} = \sum_{j=1}^{d_1} \sum_{k=1}^{d_1} \left(\frac{N}{B_3} \sum_{u \in \mathcal{B}_3} q_j(u) q_k(u) - \delta_{jk} \right)^2$, $\hat{L}_{\text{ortho2}} = \sum_{j=1}^{d_2} \sum_{k=1}^{d_2} \left(\frac{N}{B_3} \sum_{u \in \mathcal{B}_3} f_j(u) f_k(u) - \delta_{jk} \right)^2$ ($\delta_{jk} = 1$ if $j = k$ and $\delta_{jk} = 0$ otherwise).

When edges and nodes are observed sequentially (incrementally expanding Ω), neural network parameters θ can be efficiently updated without recomputing the full eigendecomposition, enabling effective online graph optimization and scalability to dynamically growing graphs.

4.2 Global Graph Bayesian Optimization using Spectral Embedding

We now present the global BO framework tailored for graphs, leveraging spectral embeddings and GP modeling.

4.2.1 Spectral kernel for Gaussian processes.

Given the node embeddings $f(u) \in \mathbb{R}^{d_2}$ learnt from solving problem (6), we construct a GP model to capture the relationships between node embeddings and their corresponding function values. Unlike conventional Euclidean kernels, we define our kernel explicitly in terms of the spectral decomposition of the graph Laplacian:

$$k(u, v) = \sum_{i=1}^{d_2} r(\lambda_i) \phi_i(u) \phi_i(v),$$

where the normalized embeddings are $\phi(u) = \frac{f(u)}{\|f(u)\|_2}$, $\{\lambda_i\}_{i=1}^{d_2}$ are the d_2 smallest non-zero eigenvalues of \tilde{L} , calculated via the Rayleigh quotient $\lambda_i = \frac{f_i^\top \tilde{L} f_i}{f_i^\top f_i}$. The function $r(\lambda_i)$ is a spectral filter controlling the contribution of each eigen-component. Common examples include the polynomial filter $r(\lambda_i) = \sum_{\alpha=0}^{\eta-1} \beta_\alpha \lambda_i^\alpha + \epsilon$, or the Matérn-type filter $r(\lambda_i) = (\beta\nu + \lambda_i)^{-\nu}$, usually used for smooth interpolation on graphs. This spectral kernel naturally induces a reproducing kernel Hilbert space (RKHS) where smoothness of functions respects the intrinsic graph geometry encoded by the Laplacian spectrum.

Table 1: Optimality gap on different graphs during the optimization, with the mean optimality gap ($\pm 95\%$ CI) after 200 iterations, averaged over 10 runs. Our global BO method is instantiated with three spectral kernels (polynomial, RBF, and Matérn).

Graph Type	Max	Random	Local	BFS	DFS	Local BO	Ours (Poly)	Ours (RBF)	Ours (Matérn)
SBM-1000	1.57	0.49 ± 0.30	0.57 ± 0.17	0.83 ± 0.24	0.78 ± 0.35	0.42 ± 0.20	0.04 ± 0.07	0.04 ± 0.08	0.05 ± 0.08
SBM-2000	2.28	1.11 ± 0.62	0.79 ± 0.42	1.77 ± 0.37	1.63 ± 0.31	1.15 ± 0.50	0.04 ± 0.07	0.06 ± 0.08	0.06 ± 0.08
RDPG-1000	2.00	1.36 ± 0.54	1.13 ± 0.22	0.50 ± 0.00	0.50 ± 0.00	1.02 ± 0.32	0.06 ± 0.01	0.05 ± 0.01	0.05 ± 0.01
RDPG-2000	2.15	1.51 ± 0.58	0.56 ± 0.39	1.63 ± 0.47	1.77 ± 0.39	0.68 ± 0.53	0.06 ± 0.07	0.05 ± 0.01	0.05 ± 0.01
Ego-Facebook ¹	0.76	0.64 ± 0.03	0.19 ± 0.16	0.25 ± 0.22	0.35 ± 0.22	0.16 ± 0.13	0.06 ± 0.03	0.04 ± 0.03	0.05 ± 0.03

¹ Values are in units of 10^{-2} .

4.2.2 GP likelihood and hyperparameter estimation.

Given observed function values $\mathbf{y} \in \mathbb{R}^{|\mathcal{V}^{(t)}|}$ at nodes $\mathcal{V}^{(t)}$, the GP negative log marginal likelihood is:

$$\begin{aligned} \mathcal{L}_3(\mathbf{y} \mid \mathbf{f}, \boldsymbol{\lambda}, \boldsymbol{\beta}) &= \frac{1}{2} \mathbf{y}^\top (K + \sigma^2 I)^{-1} \mathbf{y} \\ &+ \frac{1}{2} \log \det(K + \sigma^2 I) + \frac{|\mathcal{V}^{(t)}|}{2} \log(2\pi), \end{aligned}$$

where the covariance matrix $K \in \mathbb{R}^{|\mathcal{V}| \times |\mathcal{V}|}$ has entries $K_{uv} = k(u, v)$, and σ^2 denotes observation noise variance. When observations are assumed noiseless, we set $\sigma^2 = 0$. Hyperparameters $\boldsymbol{\beta}$ of the spectral filter and noise variance σ^2 can be tuned via maximum marginal likelihood estimation (MLE), typically using gradient-based optimization.

4.2.3 Acquisition functions for node selection.

Given the fitted GP model, we choose the next node to query based on an acquisition function. Several strategies exist, including Expected Improvement (EI), Upper Confidence Bound (UCB), and Thompson Sampling [2], each balancing exploration (querying uncertain nodes) and exploitation (querying nodes with promising predicted values). We specifically employ the EI acquisition function due to its widespread effectiveness in BO, defined as:

$$\alpha_{\text{EI}}(v) = \begin{cases} 0, & \text{if } \sigma(v) = 0, \\ (y^* - \mu(v)) \Phi\left(\frac{y^* - \mu(v)}{\sigma(v)}\right) + \sigma(v) \phi\left(\frac{y^* - \mu(v)}{\sigma(v)}\right), & \text{o.w.} \end{cases}$$

where $y^* = \max_{u \in \mathcal{V}^{(t)}} y(u)$ is the current best observed value, $\mu(v)$ and $\sigma(v)$ are the GP predictive mean and standard deviation at node v , and ϕ and Φ are the probability density and cumulative distribution functions of the standard normal distribution.

Thus, the next node selected for evaluation is:

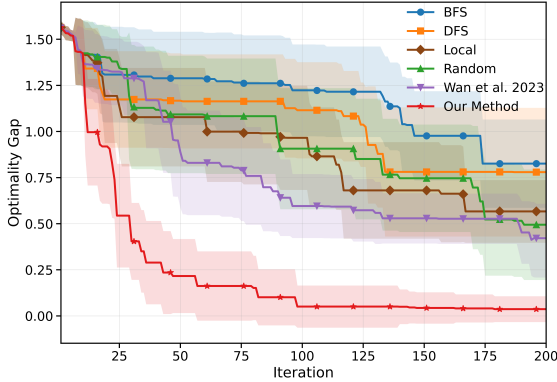
$$v^{(t+1)} = \arg \max_{v \in \mathcal{V}} \alpha_{\text{EI}}(v).$$

This process iteratively refines the graph model and optimization, adaptively guiding exploration towards globally optimal nodes based on spectral embeddings and Gaussian Process modeling. The detailed step-by-step procedure of our proposed global graph BO framework is summarized in Algorithm 1.

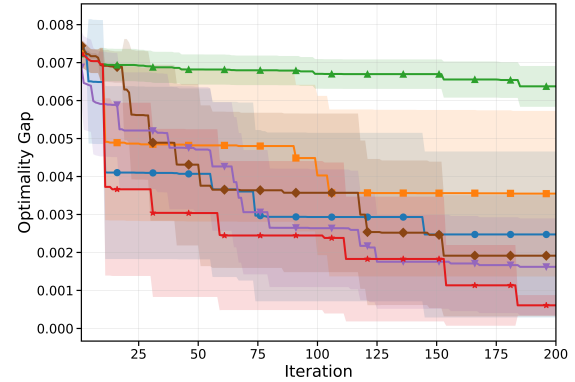
5 Experiments

5.1 Experimental Setup

We compare our method against five baseline approaches on synthetic and real-world graphs. These baselines include: (1) heuristic random sampling, (2) local search methods, (3) breadth-first search (BFS) sampling, (4) depth-first



(a) Stochastic Block Model (SBM) graphs with 1000 nodes.



(b) Ego-Facebook network with 4039 nodes.

Figure 2: Comparisons of optimization convergence with 95% confidence intervals.

search (DFS) sampling, and (5) local graph BO from a state-of-the-art work [1]. We evaluate using our spectral BO with polynomial, RBF, and Matérn kernels. All methods are run under the same graphs, with the same initial budget of 10 random node value observations. We measure performance using the simple regret/optimality gap $r_t = y(v^*) - \max_{v \in \mathcal{V}(t)} y(v)$, where $y(v^*)$ is the global maximum. Performance is averaged over 10 independent runs.

Experiments were conducted on NVIDIA A6000 GPU. We train the neural network in our method using the Adam optimizer with learning rate $(\eta_Q, \eta_\Gamma, \eta_F) = 10^{-3}, 5 \times 10^{-4}, 10^{-3}$, regularization weights $(\tau, \mu_2, \mu_Q, \mu_F) = (0.5, 0.5, 0.1, 0.1)$, GP learning rate 10^{-2} , and batch sizes $(B_1, B_2, B_3) = (128, 256, 256)$. Table 1 and Figs. 2 summarizes the optimization performance of all methods across all graph types, reporting the mean optimality gap ($\pm 95\%$ CI) after 200 iterations.

5.2 Synthetic Graphs

We evaluate our method on both synthetic and real-world graphs to demonstrate its effectiveness across diverse graph structures and properties. For synthetic experiments, we generate synthetic graphs based on Stochastic Block Model (SBM) and Random Dot Product Graph (RDPG) with varying graph structures.

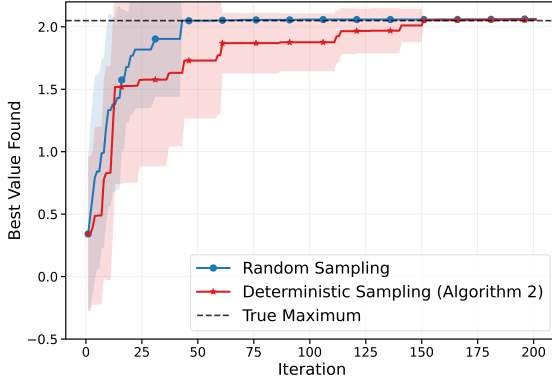
For each graph type, we test on networks with $n \in \{1000, 2000\}$ nodes. Edge weights are sampled uniformly from $[0, 1]$. we construct bandlimited signals $y : V \rightarrow \mathbb{R}$ using the first $k = 10$ eigenvectors of the graph Laplacian: $f = \sum_{i=1}^k \alpha_i \phi_i$, where $\alpha_i \sim \mathcal{N}(0, 1)$ and ϕ_i is the i -th normalized eigenvector. This ensures the signal respects the graph's spectral structure while providing ground truth for evaluation. We consider maximizing this bandlimited signal, which is a common objective in graph optimization tasks.

5.3 Real-world Graphs

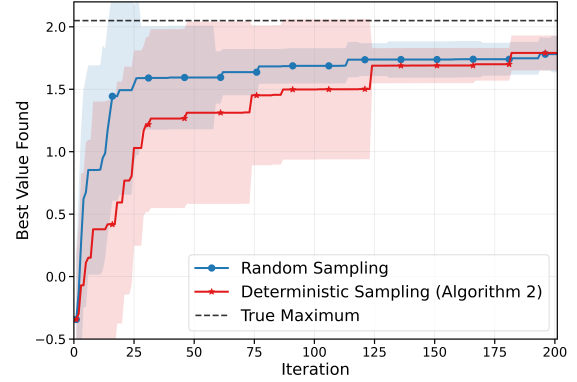
For real-world graph data, we use the Ego-Facebook network from the SNAP dataset [30, 31], containing 4,039 nodes and 88,234 edges representing social connections. We define the node function as PageRank [32], which identifies influential nodes for information propagation. This task is fundamental in viral marketing and social influence analysis. We showed our real-world results in Table 1 and Fig. 2(b). Our method obtained the minimum gap 0.04 compared to baselines.

5.4 Ablation Evaluation

We evaluate the impact of Algorithm 2 versus random edge sampling. Fig. 3 plots the optimization curves (mean $\pm 95\%$ C.I.) on two synthetic graphs. In Fig. 3(a) of low-rank RDPG, every row carries essentially similar information. Random



(a) RDPG graph of 1000 nodes with true rank 50.



(b) Power-law graph of 1000 nodes with full rank.

Figure 3: Ablation study on edge sampling method: optimization convergence with 95% confidence intervals.

edge sampling converges slightly faster, as oversampling a “seed” row gives no extra information and temporarily perturbs degree balance. In Fig. 3(b) of high-rank power-law graph, some nodes of interest (e.g., low-degree nodes or high-degree hubs) matter disproportionately. The proposed balanced deterministic edge sampling first attaches the seed to under-sampled low-degree nodes (lowering $\varphi_{\tilde{G}}$), then uniform re-balancing restores the spectral gap $\xi_{\tilde{G}}$. This yields an improvement in local reconstruction error without increasing the number of edge samples, and a modest improvement in global convergence finally.

The theoretical underpinning is that the uniform random sampling requirement $|\Omega| \sim \mu r n \log^2 n$ grows linearly in effective rank r . By concentrating the early budget on *nodes of interest* for edge sampling, and then re-balancing, our sampler preserves the same minimax sample complexity $\mathcal{O}(rn \log^2 n)$ while delivering faster local convergence on the focal nodes. Exact global recovery still requires $\mathcal{O}(rn \log^2 n)$ edges, yet with better early performance and lower error on focal nodes – consistent with Theorems 1–2 and Remark 1.

We also conduct an ablation study examining the impact of rank budget d_1 and embedding dimension d_2 on optimization performance. By increasing d_1 from 20 to 100, we observe improved graph reconstruction accuracy with diminishing returns. Performance saturates when d_1 exceeds the intrinsic rank r of the underlying graph, as the nuclear norm penalty in Problem (1) naturally induces an effective rank matching the true low-rank structure. Increasing d_2 from 5 to 50 captures additional spectral components of the graph Laplacian, improving GP model expressiveness. However, marginal benefits diminish beyond $d_2 = 10$ for our bandlimited test functions constructed from the first 10 eigenvectors, as the signal bandwidth is effectively captured. This is further detailed in the ablation study in the appendix.

6 Conclusion

We introduced a novel framework for global Bayesian optimization on graph-structured domains with partially observed topology. By leveraging low-rank matrix completion and spectral graph embedding, our method constructs a principled Gaussian process surrogate, enabling efficient global search and uncertainty quantification even from sparse graph observations. We provide rigorous theoretical guarantees for exact graph recovery under both random and deterministic sampling regimes, alongside scalable neural network-based parameterizations for efficient, online learning of graph structure and embeddings. Extensive experiments on synthetic and real-world graphs demonstrate substantial improvements over state-of-the-art baselines.

References

- [1] Xingchen Wan, Pierre Osselin, Henry Kenlay, Binxin Ru, Michael A. Osborne, and Xiaowen Dong. Bayesian optimisation of functions on graphs. In *Advances in Neural Information Processing Systems*, volume 36, pages 43012–43040, 2023.
- [2] Peter I Frazier. A tutorial on bayesian optimization. *arXiv preprint arXiv:1807.02811*, 2018.
- [3] Jasper Snoek, Hugo Larochelle, and Ryan P. Adams. Practical bayesian optimization of machine learning algorithms. In *Advances in Neural Information Processing Systems (NeurIPS)*, 2012.
- [4] Yongsheng Mei, Mahdi Imani, and Tian Lan. Bayesian optimization through gaussian cox process models for spatio-temporal data. In *The Twelfth International Conference on Learning Representations, ICLR 2024, Vienna, Austria, May 7-11, 2024*. OpenReview.net, 2024. URL <https://openreview.net/forum?id=9j1RD9LlWH>.
- [5] Yongsheng Mei, Tian Lan, Mahdi Imani, and Suresh Subramaniam. A bayesian optimization framework for finding local optima in expensive multimodal functions. In *ECAI*, 2023.
- [6] Jiaxu Cui, Bo Yang, and Xia Hu. Deep bayesian optimization on attributed graphs. In *Proceedings of the AAAI Conference on Artificial Intelligence*, volume 33, pages 1377–1384, 2019.
- [7] Binxin Ru, Xingchen Wan, Xiaowen Dong, and Michael Osborne. Interpretable neural architecture search via bayesian optimisation with weisfeiler–lehman kernels. *arXiv preprint arXiv:2006.07556*, 2020.
- [8] Changyong Oh, Jakub M. Tomczak, Efstratios Gavves, and Max Welling. Combinatorial bayesian optimization using the graph cartesian product. In *Advances in Neural Information Processing Systems*, volume 32, 2019.
- [9] Yilin Xie, Shiqiang Zhang, Jixiang Qing, Ruth Misener, and Calvin Tsay. Global optimization of graph acquisition functions for neural architecture search. *arXiv preprint arXiv:2505.23640*, 2025.
- [10] Peter D Hoff, Adrian E Raftery, and Mark S Handcock. Latent space approaches to social network analysis. *Journal of the american Statistical association*, 97(460):1090–1098, 2002.
- [11] Santo Fortunato. Community detection in graphs. *Physics reports*, 486(3-5):75–174, 2010.
- [12] Emmanuel J. Candès and Benjamin Recht. Exact matrix completion via convex optimization. *Foundations of Computational Mathematics*, 9(6):717–772, 2009.
- [13] Raghunandan H Keshavan, Andrea Montanari, and Sewoong Oh. Matrix completion from a few entries. *IEEE transactions on information theory*, 56(6):2980–2998, 2010.
- [14] Jiaxu Cui and Bo Yang. Graph bayesian optimization: Algorithms, evaluations and applications. *arXiv preprint arXiv:1805.01157*, 2018.
- [15] Dhanesh Ramachandram, Michal Lisicki, Timothy J. Shields, Mohamed R. Amer, and Graham W. Taylor. Bayesian optimization on graph-structured search spaces: Optimizing deep multimodal fusion architectures. *Neurocomputing*, 298:80–89, 2018. doi: 10.1016/j.neucom.2017.11.071.
- [16] Colin White, Willie Neiswanger, and Yash Savani. Bananas: Bayesian optimization with neural architectures for neural architecture search. In *Proceedings of the AAAI Conference on Artificial Intelligence*, volume 35, 2021.
- [17] Huidong Liang, Xingchen Wan, and Xiaowen Dong. Bayesian optimization of functions over node subsets in graphs. In *Advances in Neural Information Processing Systems*, volume 37, pages 38199–38234, 2024.

[18] Zirui Yuan, Minglai Shao, and Zhiqian Chen. Graph bayesian optimization for multiplex influence maximization. In *Proceedings of the AAAI Conference on Artificial Intelligence*, volume 38, pages 22475–22483, 2024.

[19] Yilin Xie, Shiqiang Zhang, Jixiang Qing, Ruth Misener, and Calvin Tsay. Bogrpe: Bayesian optimization over graphs with shortest-path encoded. arXiv preprint arXiv:2503.05642, 2025.

[20] Emmanuel J Candès and Terence Tao. The power of convex relaxation: Near-optimal matrix completion. *IEEE transactions on information theory*, 56(5):2053–2080, 2010.

[21] Hanbyul Lee, Rahul Mazumder, Qifan Song, and Jean Honorio. Matrix completion from general deterministic sampling patterns, 2023. URL <https://arxiv.org/abs/2306.02283>.

[22] Mikhail Belkin and Partha Niyogi. Laplacian eigenmaps for dimensionality reduction and data representation. *Neural computation*, 15(6):1373–1396, 2003.

[23] Andrew Ng, Michael Jordan, and Yair Weiss. On spectral clustering: Analysis and an algorithm. *Advances in neural information processing systems*, 14, 2001.

[24] Ronald R Coifman and Stéphane Lafon. Diffusion maps. *Applied and computational harmonic analysis*, 21(1):5–30, 2006.

[25] Kondor Risi Imre. Diffusion kernels on graphs and other discrete input spaces. In *Proc. 19th Int. Conf. Machine Learning*, 2002, 2002.

[26] Alexander J Smola and Risi Kondor. Kernels and regularization on graphs. In *Learning theory and kernel machines: 16th annual conference on learning theory and 7th kernel workshop, COLT/kernel 2003, Washington, DC, USA, august 24-27, 2003. Proceedings*, pages 144–158. Springer, 2003.

[27] Yifan Wu, George Tucker, and Ofir Nachum. The laplacian in rl: Learning representations with efficient approximations, 2018. URL <https://arxiv.org/abs/1810.04586>.

[28] Yuu Jinnai, Jee Won Park, Marlos C. Machado, and George Konidaris. Exploration in reinforcement learning with deep covering options. In *International Conference on Learning Representations*, 2020. URL <https://openreview.net/forum?id=SkeIyaVtwB>.

[29] Carl Eckart and Gale Young. The approximation of one matrix by another of lower rank. *Psychometrika*, 1(3):211–218, 1936.

[30] Julian McAuley and Jure Leskovec. Learning to discover social circles in ego networks. In *Advances in Neural Information Processing Systems (NIPS)*, 2012.

[31] Julian McAuley and Jure Leskovec. Facebook ego network dataset – snap (stanford network analysis project). <https://snap.stanford.edu/data/egonets-Facebook.html>, 2012. Accessed: July 1, 2025.

[32] Lawrence Page, Sergey Brin, Rajeev Motwani, and Terry Winograd. The pagerank citation ranking: Bringing order to the web. Technical report, Stanford infolab, 1999.